Mutual Interference and Low Probability of Interception Capabilities of Noise Radar

Thayananthan Thayaparan, Miloš Daković, LJubiša Stanković

Abstract— **Recently, there has been considerable interest in noise radar over a wide spectrum of applications, such as through-wall surveillance, tracking, Doppler estimation, polarimetry, interferometry, ground-penetrating or subsurface profiling, detection, synthetic aperture radar (SAR) imaging, inverse synthetic aperture radar (ISAR) imaging, foliage penetration imagging, etc. Major advantages of using noise in the transmit signal are its inherent immunity from radio frequency and electromagnetic interference, improved spectrum efficiency, and hostile jamming as well as being very difficult to detect. In this paper, the basic theory of digital signal processing in noise radar design is presented. The theory supports the use of noise waveforms for radar detection and imaging in such applications as covert military surveillance and reconnaissance. It is shown that by using wide-band noise waveforms, one can achieve high range resolution and reduced range estimation ambiguity. Mutual interference and low probability of interception (LPI) capabilities of noise radar are also evaluated. The simulation results show the usefulness of the noise radar technology to improve on conventional radars.**

I. Introduction

The term "random noise" as applied to radar refers to techniques and applications that use incoherent noise as the probing transmit waveform. Noise radar is a form of random signal radar that employs incoherent noise as the probing transmit waveform in contrast to the conventional pulse, CW (continuous wave), FM (frequency modulated), or FM/CW radars. Because of the truly random transmitting signal, noise radars have many advantages when compared with conventional radars, including unambiguous estimation of range, high immunity to noise, low probability of intercept (LPI), high electro-magnetic compatibility, good electronic counter countermeasure (ECCM) capability, good counter electronic support measure (CESM) capability, and ideal 'thumbtack' ambiguity function [1]-[25]. Noise radar systems have not yet reached sufficient maturity for military use. The objective of this paper is to make clear the advantageous effects of noise radar in current and for future military applications.

The research on noise radar or random signal radar started in 1960s [5]. At that time, theoretical analysis was made and some prototypes were constructed. However, due to the limited availability of suitable electronic components, the research on noise radar dropped quickly, for the following reasons: 1) while generation of pseudorandom signals had been well developed, generation of pure random signals was not achievable at that time; 2) for noise radar, modulation of a transmitting signal is random. So the correlation processing is necessary instead of the common pulse compressor. Therefore, microwave variable delay-line is a key component in the receiver of noise radar. However, the manufacturing of microwave variable delay-lines was also very difficult and expensive to do in the past. Since 1990, the development of solid-state microwave components and high-speed VLSI (very large scale integration) has enabled the generation of a microwave random signals and the manufacture of microwave variable delay-lines. This technical progress most likely ensures the implementation of noise radar in the near future. Thus, the research on noise radar has increased and more required. Owing to electronic jamming in modern war, much more attention is being paid to noise radar be-

IET Radar, Sonar and Navigation, Vol. 2, No. 4, Aug. 2008.

cause of its good ECCM and CESM properties. An all-around review of noise radar or random signal radar in the past thirty years is given in [11]-[12].

Over the past few years, the research has been devoted to the development and implementation of random noise radar by various research groups [4], [8], [13]-[17]. Recent research has investigated the potential use of noise radar for ultrawideband SAR/ISAR imaging, Doppler and polarimetric measurements, collision warning, detection of buried objects, and targets obscured by foliage [2], [6], [15]-[25]. Wide bandwidth gives high range resolution, and the extended pulse length improves the transmitted average power. The non-periodic waveform suppresses the range ambiguity while reducing the probability of intercept and interference. The implementations of varying complexity of noise radar were analyzed and discussed in [1]-[25].

In this paper, we describe the correlation based processing of noise radar returns. In this case, a part of the transmitted signal is used as a reference. When a radar return is received, it is down-converted to the IF-band coherently using the reference signal. This method makes use of a digital delay line to delay the reference signal before multiplying it by the IF radar return. The resulting product is passed through a low pass filter to produce a correlation function of the product. The range of a target is estimated as the time delay given by the position of the correlation function's maximum [1]-[2], [4], [6]. We derive correlation functions for such a receiver based on a variety of transmitted signals and present results from simulations of specific radar systems.

An important operational consideration of all radar systems is mutual interference. In order to provide results concerning mutual interference, we examine the case when multiple noise radars are operating simultaneously. These results are compared to those obtained by conventional radars employing a linear frequency modulated (LFM) waveform. Also, more specific to the application of covert surveillance, is the low probability of interception performance of noise radar systems. In this paper, we compare noise radars with conventional LFM radars in terms of the ability of ESM systems to detect either one in various noisy environments.

II. Theoretical background

There exist many approaches to the realization of noise radars [1], [2]. The transmitted and returned signals from noise radars are wideband high-frequency signals. These signals can be processed at high frequencies or translated to the baseband before analog, digital and combined processing algorithms can be performed. In the rest of the paper we will assume that the transmitted and received signals are translated to baseband and are adequately sampled prior to further processing.

A. Correlation Receiver

The correlation uses the principle that when the delayed reference signal is correlated with the actual target echo, the peak value of the correlation process can indicate the distance to the target (the amount of time delay of the reference signal is also a measure of distance to the target), while outputs of Doppler filters following the correlator give target velocity [8]. Figure 1 shows the main elements of random noise radar. A noise signal is transmitted, and a delayed signal is received from a point target. A replica of the transmitted noise, delayed by T_0, is correlated with the received signal. When T_r is varied a strong correlation peak is obtained for $T_r = T_0$, which gives an estimate of the target range $r_0 = cT_0/2$.

Let us consider a radar emitting a time limited signal $x(t)$. Denote the received signal by $y(t)$. Furthermore, we assume that a single point scatterer is located at the range r_0 along the radar line-of-sight (LOS). According to this assumption, the received signal can be written as:

$$y(t) = A_\sigma x(t - T_0) + \varepsilon(t) \tag{1}$$

where $T_0 = 2r_0/c$ is the round-trip delay caused by the finite speed of the electromagnetic waves, $\varepsilon(t)$ is an undesired part of the received signal (noise caused by the reflection from other objects along the LOS) and A_σ denotes target reflectivity. Without loss of gen-

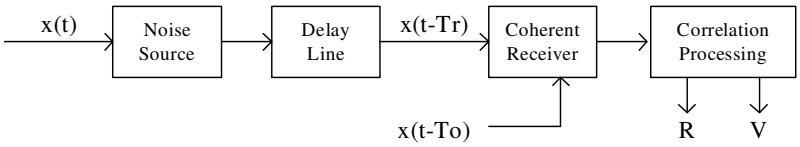

Fig. 1. Main components of noise radar with external delay line.

erality we will assume that $A_\sigma = 1$. The correlation of the emitted and received signals can be written as:

$$R(\tau) = \int_0^{T_{int}} y(t)x^*(t-\tau)dt. \qquad (2)$$

where T_{int} is the integration time. In the noiseless case, the maximum value of $|R(\tau)|$ is at the point $\tau = T_0$.

Let us now assume that $x(t)$ is a white stationary Gaussian random process with autocorrelation function $R_{xx}(\tau)$. The output of the correlation receiver given by (2) is also a random process. Let us analyze the expected value of (2) as:

$$\begin{aligned} E[R(\tau)] &= E[\int_0^{T_{int}} y(t)x^*(t-\tau)dt] \\ &= \int_0^{T_{int}} E[y(t)x^*(t-\tau)]dt \\ &= \int_0^{T_{int}} (E[x(t-T_0)x^*(t-\tau)] \\ &\quad +E[\varepsilon(t)x^*(t-\tau)])\,dt \\ &= \int_0^{T_{int}} R_{xx}(\tau-T_0)dt \\ &\quad + \int_0^{T_{int}} E[\varepsilon(t)x^*(t-\tau)]dt \quad (3) \end{aligned}$$

If the emitted signal $x(t)$ and the noise $\varepsilon(t)$ are independent processes then the second term in (3) is equal to zero and we get:

$$E[R(\tau)] = T_{int}R_{xx}(\tau - T_0). \qquad (4)$$

Since the autocorrelation function's maximum is at $u = 0$ ($R(\tau) \leq R(0)$), the delay T_0 can be estimated as the position of the maximum as:

$$T_0 = \max_\tau |E[R(\tau)]| \qquad (5)$$

Special cases:

- Let $x(t)$ be the white stationary Gaussian random process. The autocorrelation function is $R_{xx}(\tau) = I_0\delta(t-\tau)$. This is an ideal shape since $E[R(\tau)] = T_{int}I_0\delta(t-\tau)$, and its maxima are ideally defined (only one point is different from zero). Note that signals of this form are not bandlimited and they can not be used in practical applications.
- Let $x(t)$ be the bandlimited white stationary Gaussian random process with power spectral density (PSD) $S_{xx}(f) = S_0$ for $f_0 - B/2 \leq f < f_0 + B/2$ and $S_{xx}(f) = 0$ otherwise. The autocorrelation function is of the form:

$$R_{xx}(\tau) = S_0 e^{j2\pi f_0 \tau} \frac{\sin(\pi B\tau)}{\pi\tau} \qquad (6)$$

with well defined maxima at $\tau = 0$, but also with side lobes. The first side lobe is $B\frac{\pi}{2}$ times lower than the main maximum.

B. Implementation issues

The first step is the generation of noise sequence. We will assume that the noise is a white complex Gaussian noise with independent real and imaginary parts and unity variance. The noise sequence length N depends on the time duration of the transmitted signal T_{int} and its bandwidth B

$$N = [T_{int}B]$$

Note that the signal duration is referenced as "pulse repetition time" as in the radar with deterministic (and periodic) waveforms, but in the noise radar case, there is no repetition time since the transmitted waveform is different at each dwell. It should be noted that the high bandwidth (required for good range resolution) increases the number of samples and consequently the computational time.

The transmitted noise sequence is denoted as $x(n)$. The transmitted signal is a modulated

noise sequence $x_t(t) = e^{j2\pi f_0 t}x(t)$ where $x(t)$ is an output of the D/A converter excited with random discrete sequence $x(n)$.

The second step is to determine the received signal reflected from the moving target at the range r_0 and velocity along the radar line of sight v_0. The time delay of the received signal is $T_0 = \frac{c}{2(r_0+v_0 t)}$. Note that in the case of moving target the time delay is time dependent. The received signal in analog domain is

$$y(t) = Ax_t(t - T_0) = Ae^{j2\pi f_0(t-T_0)}x(t - T_0)$$

where the signal amplitude A is proportional to the target reflectivity and inversely proportional to the square of the target range r_0^2. After the translation to the baseband, the received signal becomes

$$y_{bb}(t) = Ae^{-j2\pi f_0 T_0}x(t - T_0)$$

In the discrete domain, the above relation is implemented by delaying the input sequence $x(n)$ by $n_0 = [BT_0]$ samples and applying the linear interpolation in order to improve the delay accuracy as mentioned in the previous subsection. The discrete received sequence will then be denoted as $y(n)$.

In the next step the convolution $c(n)$ of the original sequence $x(n)$ and the received sequence $y(n)$ is performed. In order to lower the computational complexity, an FFT is applied in the convolution computation

$$c(n) = FFT^{-1}\left[FFT[y(n)] \cdot FFT[x(n)]^*\right]$$

The single transmitted pulse gives the information for the target range. There will be a strong peek in the correlation sequence $c(n)$. The peek position n_{cp} can be converted into range

$$r_{est} = n_{cp}\Delta r = n_{cp}\frac{c}{2B} = \frac{n_{cp}}{N}cT_{int}.$$

The maximal observable range is obtained for $n_{cp} = N$ and is equal to

$$r_{\max} = cT_{int}.$$

Note that targets at range higher than $r_{\max}$ do not introduce ambiguity. Such returns are treated as noise and they are spread over all samples of $c(n)$.

In order to estimate the target velocity the above procedure is repeated M times, i.e. M pulses are transmitted and M returns are processed. The obtained correlation sequences are denoted as $c_m(n)$ where m stands for pulse index. The Doppler estimation is performed in the conventional way, i.e., by performing FFTs on the observed correlation sequences with respect to the pulse index m. We will then observe the strong peak at the position m_{cp} which can be converted into target velocity as

$$v_{est} = m_{cp}\frac{c\pi}{2\pi f_0 MT_{int}} = \frac{m_{cp}}{M}\frac{c}{2f_0 T_{int}}$$

Note that the velocity can be positive or negative so that m_{cp} can take values from $-M/2$ to $M/2 - 1$. The maximum unambiguous target velocity is

$$v_{\max} = \frac{c}{4f_0 T_{int}}$$

If the target velocity is higher than $v_{\max}$, then the estimated velocity will be ambiguous.

Random signal generation: There exist a few approaches to the generation of random signal. Thermal noise and dedicated microwave noise devices (hardware noise generators) are almost ideal choices. Another approach uses chaotic oscillators. Lastly, pseudo-random number generators (software noise generators), which are easiest to implement in fully digital systems.

The main advantage of the noise radar sequence is that the sequence is not periodic. It is a fact that hardware noise generators do not produce periodic sequences. Pseudo random number generators (PRNG) are inherently periodic, with a very long period. The random sequence period depends on initial condition of the PRNG (seed), and it is very important that PRNG has a long enough period for an arbitrary seed. As an example 128 bit PRNG has a theoretical maximal sequence length of $2^{128} \approx 3.4{\cdot}10^{38}$. If we assume that one random number is generated every 0.1 ns, the sequence will repeat after $1.14 \cdot 10^{21}$ years. However in practice PRNG sequence length will be much smaller for badly chosen seeds. In this paper

we will use the pseudorandom noise generator implemented in MATLAB to generate noise sequences.

Digital delay line: Since all simulations are implemented in the discrete domain, the delay line is also implemented digitally. The received signal is delayed by time T_0 (Figure 1). Let us denote the bandwidth of the transmitted and received signal with B and assume that the critical sampling is performed $T_s = \frac{1}{B}$. Now the discrete time delay can be expressed as the number of delay samples

$$n_0 = \left[\frac{T_0}{T_s}\right] = [BT_0]$$

where $[\cdot]$ stand for nearest integer. Note that in this way we can not implement the true time delay T_0 but only the discrete time delays nT_s. This approximation assumes that the target is always located in the center of the considered range cell.

Further improvements of the delay line can be performed by approximating the noninteger discrete time delays using some form of interpolation. We used a linear interpolation function to obtain the delayed signal without assuming that the target lies in the center of the range cell. This introduces an approximation error since the linear interpolation between two noise samples is not always the true time delay of the input signal.

Example: Let us assume that the transmitted and received signals are demodulated to the baseband $-B/2 \leq f < B/2$. In this case, according to the sampling theorem, we must have $N = BT_{int}$ samples within one pulse. $x(n)$ denotes the samples of the transmitted signal and $y(n)$ denotes the samples of the received signal. We can then calculate the correlation in the discrete domain as:

$$R(k) = \sum_{n=0}^{N-1} y(n)x^*(n-k) \qquad (7)$$

and the maximum of $R(\tau)$ is estimated with discrete step $\Delta\tau = \frac{T_{int}}{N} = \frac{1}{B}$ and the range resolution will be $\Delta r = \frac{c}{2B}$, as in the case of conventional radars.

Note that the number of range cells, i.e. the range of the index k in (7) can be less than N. Namely if we define the maximum target range $r_{\max}$ then we should use $k = 0, 1, ..., k_{\max}$, and $k_{\max} = \frac{r_{\max}}{\Delta r} = N\frac{2r_{\max}}{T_{int}c}$ can be significantly less than N. This can significantly reduce the computational load on the correlation receiver, which in turn can strengthen its usefulness in an operational situation for short-range applications.

The fast Fourier transform (FFT) can be used for the calculation (7). Note that in this case we obtain N samples of $R(\tau)$, so if $k_{\max} \ll N$ we will have many unnecessary calculations.

In this example we use the radar carrier frequency $f_0 = 10\,\text{GHz}$, bandwidth $B = 51.2$ MHz, and pulse repetition frequency PRF = 1000 kHz. The number of samples within the radar pulse is $N = BT_{int} = 512$. The range resolution is $\Delta r = \frac{c}{2B} = 2.93\,\text{m}$, and the maximum range is $r_{\max} = N\Delta r = 1500\,\text{m}$. There are three stationary targets simulated along the LOS (line-of-sight) at $r_1 = 100\,\text{m}$, $r_2 = 400\,\text{m}$ and $r_3 = 500\,\text{m}$. The correlation $R(k)$ is calculated according to the equation (11) and the results are presented in Figure 2. Figure 2 clearly shows that there are three strong correlation peaks located at the expected ranges. Note that there are no noticeable sidelobes.

III. Mutual Interference

When two or more radar systems operate in close proximity at the same frequency band, they could produce a scenario where mutual interference (MI) is experienced.

In the presented model, we assume that there are N_R continuous radars with random waveforms operating simultaneously at the same frequency band. We will consider the simplest scenario of a single-point target. Each radar transmits a signal $x_i(t)$ where $i = 1, 2, \ldots N_R$. At the receiver of the k-th radar, the received signal is of the form:

$$\begin{aligned} y_k(t) \;=\; & K_{1,k}x_1(t - t_{d,1,k}) \\ & + K_{2,k}x_2(t - t_{d,2,k}) + \ldots \\ & + K_{k,k}x_k(t - t_{d,k,k}) + \ldots \\ & + K_{N_R,k}x_{N_R}(t - t_{d,N_R,k}) + \varepsilon(t) \end{aligned} \qquad (8)$$

Time delays $t_{d,i,k}$ are proportional to the total distance $(r_{i,k})$, i.e. from the i-th radar

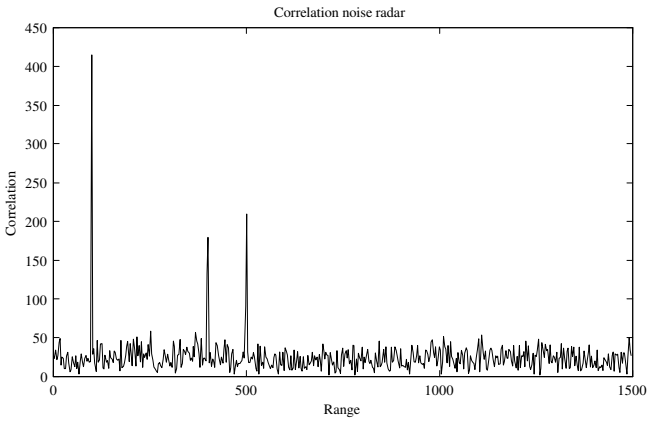

Fig. 2. Correlation receiver example (three targets located at $r_1 = 100\,\mathrm{m}$, $r_2 = 400\,\mathrm{m}$ and $r_3 = 500\,\mathrm{m}$).

to the target and then from the target to the k-th radar. Amplitude coefficients, $K_{i,k}$, are proportional to the target reflectivity and to $r_{i,k}^{-2}$. The noise level at the receiver side is $\varepsilon(t)$. It is obvious that components like $K_{k,k}x_k(t - t_{d,k,k})$ of the received signal $y_k(t)$ are of interest where all other components represent interference.

Since all radars in the scenario use a noise waveform, we can calculate the equivalent noise at the receiver and model the received signal as:

$$y_k(t) = K_{k,k}x_k(t - t_{d,k,k}) + \varepsilon_{eq}(t) \qquad (9)$$

where the power of the equivalent noise $\varepsilon_{eq}(t)$ is equal to the sum of the powers of each interference return and the power of noise $\varepsilon(t)$. The returned signal is processed by the correlation receiver as described in the previous section.

A. Mutual Interference Simulation

In this simulation three noise radars are considered. The target and radar positions are shown in Figure 3. The first and second radars are located at the same position, while the third radar is shifted. All three radars operate at 10 GHz with a 25 MHz bandwidth. The PRF for the first and third radars is 97.7 kHz and the PRF for the second radar is 116 kHz. The radar parameters are given in Table 1. It is assumed that the target moves with constant velocity 200 m/s along the first and second radars' LOS. Equations (9) and (7) are used to perform the calculations in this simulation. It should be noted that receiving antennas can pick up signals reflected from the target as well as the direct transmission from the other noise transmitters through their antenna sidelobes. The direct transmission between radars depends on the radar positions, sidelobe gains from both the receiving and transmitting antennas that depend upon the radiation patterns, and the angle between the lines-of-sight. However, in this model, we assume that the direct transmission between radars can be neglected.

Five cases with respect to the three radars' output powers are considered:

1. The three radars operate with the same power. Range Doppler profiles are shown in Figure 4. The upper row shows the radar returns of the first , second and third radars without MI (only one radar is active) while the second row shows the radar returns of the first, second and third radars with MI (all three radars are active). In this scenario, the influence of one radar on the others is negligible.
2. The first radar's power is 20 dB higher than the third radar's power, while the second radar's power is 3 dB higher than the third one. Results are shown in Figure 4. The third row shows the radar returns of the first, second and third radars with MI (all three radars are active).
3. The first radar's power is 30 dB higher

TABLE I
RADAR PARAMETERS

Radar Number	1	2	3
Operating frequency	10 GHz	10 GHz	10 GHz
Bandwidth	25 MHz	25 MHz	25 MHz
Pulse repetition frequency	97.7 kHz	119 kHz	97.7 kHz
Coherent integration time	2.62 ms	2.56 ms	2.62 ms

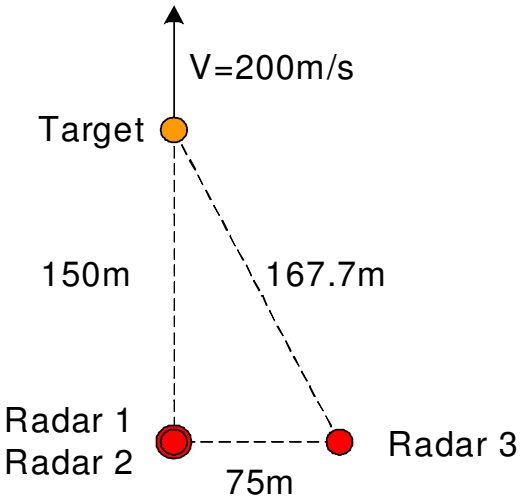

Fig. 3. Location of three radars use for simulations

than the third radar's power, while the second radar's power is 3 dB higher than the third one. Results are shown in Figure 4. The fourth row shows the radar returns of the first, second and third radars with MI (all three radars are active).

4. The first radar's power is 35 dB higher than the third radar's power, while the second radar's power is 3 dB higher than the third one. Results are shown in Figure 4. The fifth row shows the radar returns of the first, second and third radars with MI (all three radars are active). Note that the third radar is not able to detect the target.

5. The first radar's power is 40 dB higher than the third radar's power, while the second radar's power is 3 dB higher than the third one. Results are presented in Figure 4. The last row shows the radar returns of the first, second and third radars with MI (all three radars are active). The third radar is not able to detect the target.

Figure 4 shows that in all cases, the first and second radars successfully detect the target's range and velocity. In cases 4 and 5, the third radar is not able to detect either of the target's parameters because of the influence from radar 1 and radar 2 on radar 3. Another observation is that there is no significant influence from radar 2 and radar 3 on radar 1 since radar 1 has the highest transmit power. Radar 1 introduces noise in the range-Doppler profiles of the radar 2 and radar 3. These results suggest that the noise radar can operate with low SNR (up to -30 dB). However when the interference signal is 40 dB or above, the radar is not able to detect target. The interference does not introduce "ghost targets". This study indicates that for noise radars the signal transmitted from one radar is treated

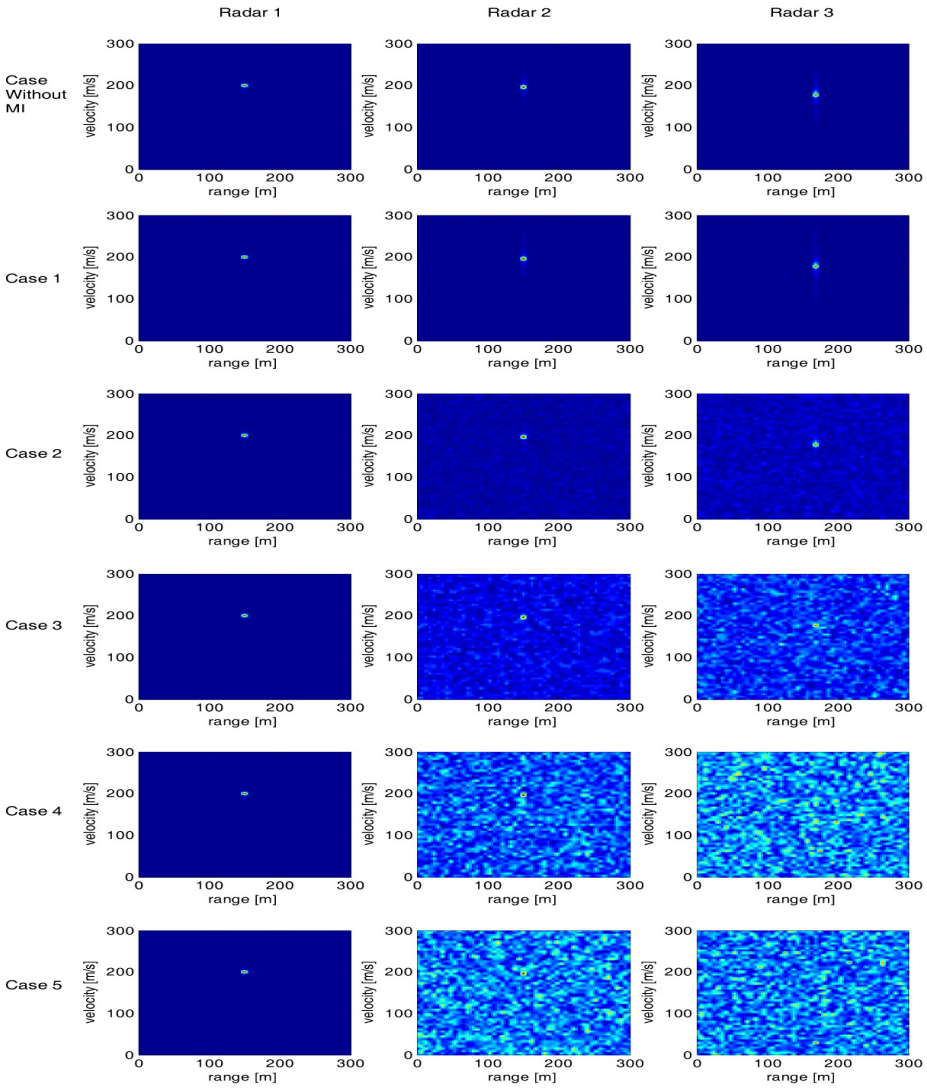

Fig. 4. Mutual interference of three radar systems

as noise for other radars, which suggests that more than one radar can share the same bandwidth. However they will effectively raise the overall noise floor.

B. Comparison Between noise radar and Conventional LFM Radar

In this section we evaluate the mutual interference effects on noise radars and linear frequency modulated (LFM) waveform radars from other such radars when determining the range and velocity of the moving target. Let us consider three X-band radars, each operating at a center frequency of 10 GHz with 150 MHz bandwidth. Assume a single-point target located at $(0\,\mathrm{m}, 0\,\mathrm{m}, 100\,\mathrm{m})$ with velocity $V_{tg} = 100\frac{\mathrm{m}}{\mathrm{s}}$. Radar locations are $(3010\,\mathrm{m}, 0\,\mathrm{m}, 0\,\mathrm{m})$ for the first radar, $(3080\,\mathrm{m}, 0\,\mathrm{m}, 0\,\mathrm{m})$ for the second radar, and $(2000\,\mathrm{m}, -2300\,\mathrm{m}, 0\,\mathrm{m})$ for the third radar. The first and third radars have the same transmit power while the transmit power of the second radar is 16 times (12 dB) higher. The target to radar distance is 3011.7 m for the first radar, 3081.6 m for the

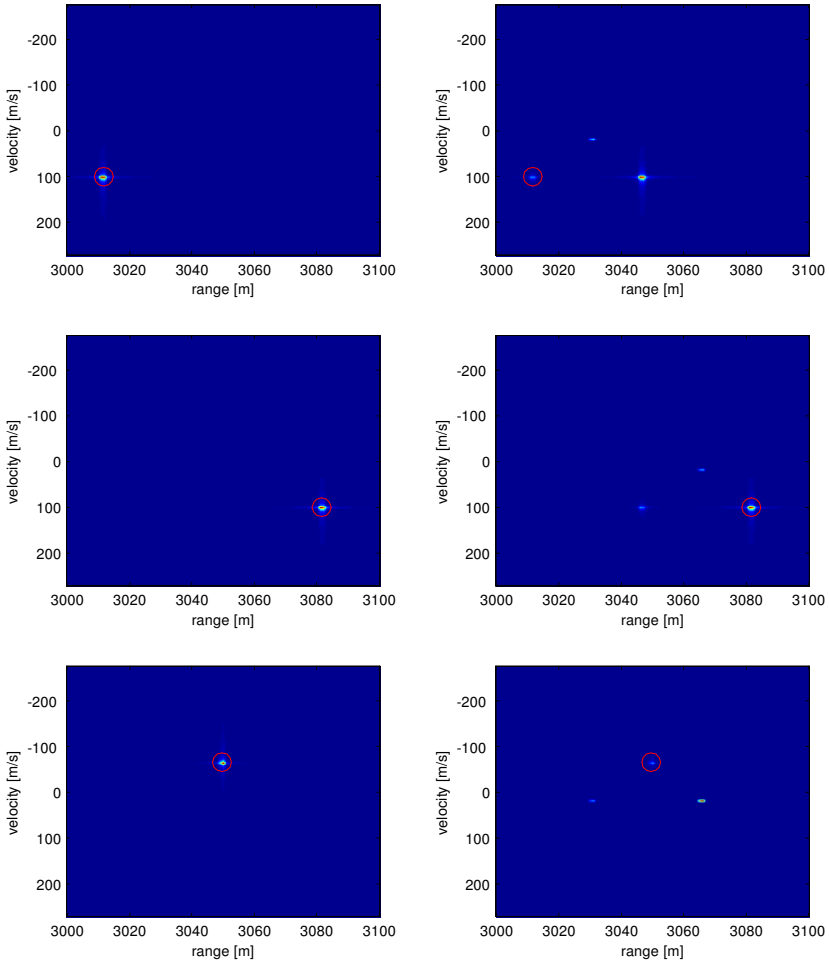

Fig. 5. Conventional LFM radars. Three radars are considered. Subplots on the left side present range-Doppler profiles when the radars operate without interference. Subplots on the right side show interference effects when the radars operate simultaneously. The second radar's transmit power is 12 dB higher than the transmit powers of the first and third radars.

second radar and 3049.6 m for the third radar. The projection of the target's velocity onto the radar LOS is $99.94\frac{\mathrm{m}}{\mathrm{s}}$ for the first radar, $99.95\frac{\mathrm{m}}{\mathrm{s}}$ for the second radar and $-65.58\frac{\mathrm{m}}{\mathrm{s}}$ for the third radar. The radars transmit a series of 128 pulses and the total integration time is 3.5 ms. The number of samples within one pulse is 4096. Note that receiving antennas can pick up signals reflected from the target as well as the direct transmission from the other noise transmitters through their antenna sidelobes. The direct transmission between radars depends on radar positions, sidelobe gains from both the receiving and transmitting antennas that depend upon the radiation patterns, and the angle between the lines-of-sight. However, in this model, we assume that the direct transmission between radars can be neglected.

Equations (9) and (7) are used to perform the calculations in this simulation.

Two cases are considered:

1. The radars' waveforms are LFM signals.
2. The radars use a random noise waveform.

The results are presented in Figure 5 for the first case and Figure 6 for the second case.

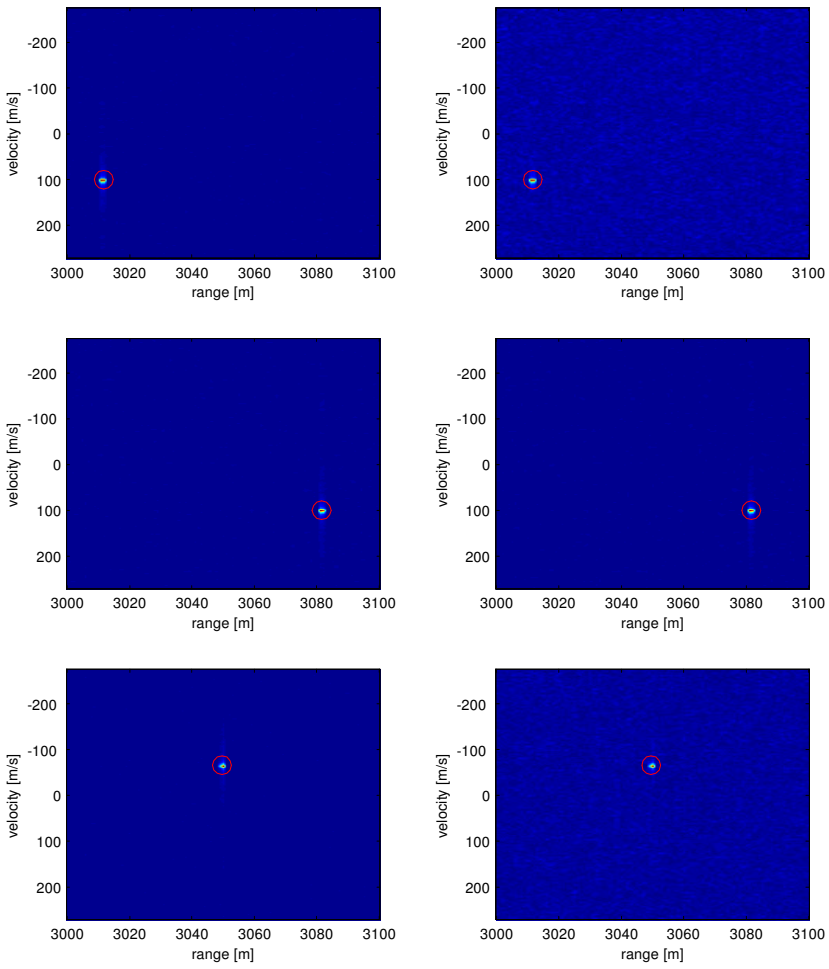

Fig. 6. Random waveform radars. Three radars are considered. Subplots on the left side present range-Doppler profiles when the radars operate without interference. Subplots on the right side show interference effects when the radars operate simultaneously. The second radar's transmit power is 12 dB higher than the transmit power of the first and third radars.

The figures consist of 6 subplots where each row corresponds to one radar. The left column plots present range-Doppler profiles for the case when only one radar is operating, while the right column plots present range-Doppler profiles for the case when all three radars are operating simultaneously.

In the conventional LFM case, only the second radar (highest power) gives a satisfactory range-Doppler profile when all radars are operating simultaneously. The first and third radar profiles result in targets with the wrong range and velocity (ghost targets).

In the noise waveform case, each radar detects the correct target parameters in solo and simultaneous operational modes. The influence of the second radar on the remaining two is expressed through a higher noise level at the receiver (first and third row, right subplots in Figure 6).

This study suggests that noise radars can operate in the same frequency band. The mutual interference involves at higher level of noise only, and can decrease the maximum detection range of the target. On the other hand, LFM radars can produce "ghost' targets when

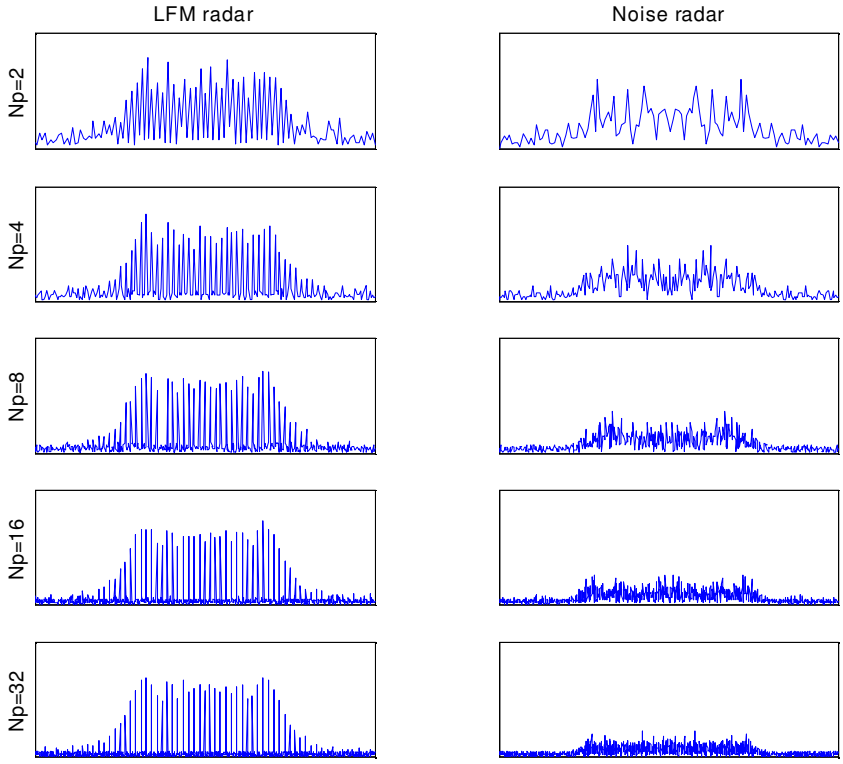

Fig. 7. Fourier spectrum of the observed signal in the case of a conventional LFM radar (left) and a NR (right) for various observation times. N_p is the number of radar pulses within the observation time. The signal to noise ratio is 10 dB.

more than one radar operate in same frequency band. The results show that noise radars are unlikely to interfere with other noise radar systems or other radar systems in the same band.

IV. Probability of Interception

Radars with conventional LFM waveforms transmit a series of identical pulses, so the easiest way to detect these radar signals is through observation over a long period of time and then examination of the Fourier spectrum of the observed signal. The decision as to whether the radar signal is present in the noise or not can be derived by comparison of the maximum value in the Fourier spectrum with some threshold level, where the threshold level should be dependent on noise. With increasing observation time, the maximum value of the Fourier spectrum can be increased within the considered frequency range significantly.

On the other hand, noise radars use stochastic waveforms and they are not periodic. The observed signal does not exploit periodicity for long observation times and the Fourier spectrum is equally distributed over the whole frequency band. That implies low probability of interception on detection of the NR signal. This heuristic analysis is presented in Figure 7 for 10 dB SNR, Figure 8 for 0 dB SNR and Figure 9 for -6 dB SNR. In this simulation, the Fourier spectrum of the observed signal in the case of a conventional LFM radar and a noise radar for various observation times are studied; N_p=2,4,8,16, and 32 radar pulses are used. There are 64 samples in each pulse. Figures 7-9 suggest that the conventional radar is easier to be detected compared with the noise radar in the same noisy environment. The obvious reason is that the deterministic waveform such as LFM involves periodicity. The periodic pulses can be detected by Fourier transform (spectrum ana-

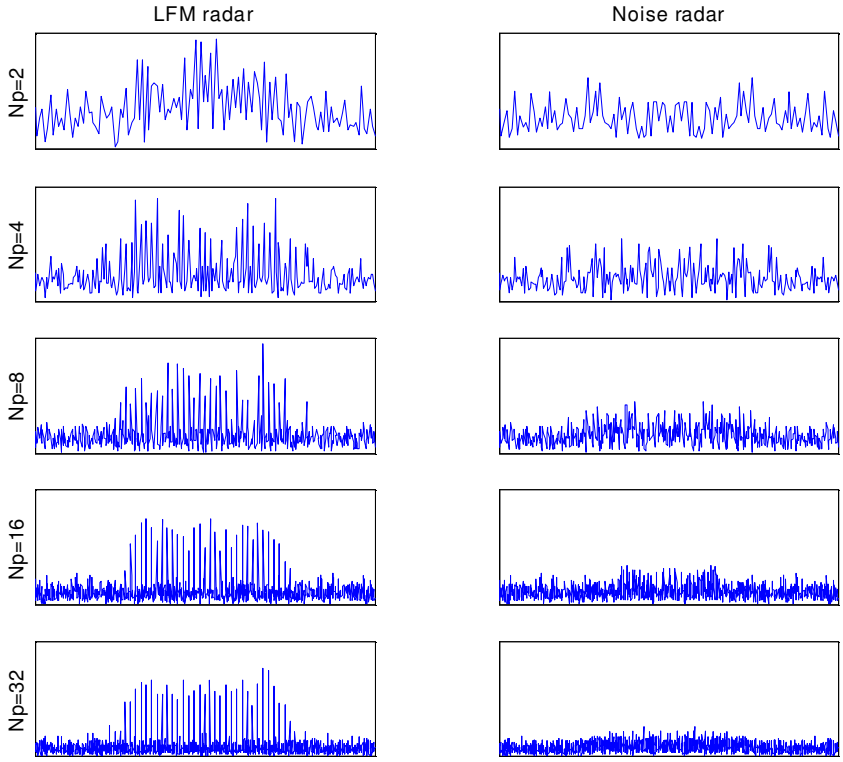

Fig. 8. Fourier spectrum of the observed signal in the case of a conventional LFM radar (left) and a NR (right) for various observation times. N_p is the number of radar pulses within the observation time. The signal to noise ratio is 0 dB.

lyzer). However stochastic waveforms are not periodic and therefore are not easy to detect by spectral analysis. The probability of interception increases rapidly when observation time increases in case of conventional LFM radar. However the probability of interception does not depend significantly on observation time in the case of random waveform radar.

V. Discussion and Conclusion

This paper presents an overview of the basic principles of noise radar technology (NRT). NRT is not currently in wide use. Only recently have achievements necessary to NRT's implementation been surfacing. The rapid advancement of digital signal processing algorithms, signal processing hardware, new methods for generation of noise waveforms, solid state microwave techniques, and integrated circuit electronics the realisation of noise radar is relatively easy. .

This paper provides theoretical and simulated-based evaluations of NRT that support its use in current and future applications. We evaluated the mutual interference effects on noise radars and linear frequency modulated (LFM) waveform radars from other radars when determining the range and velocity of the moving target. The results show that noise radars are unlikely to interfere with other noise radar systems or other radar systems in the same band. It is shown that in a variety of noisy environments, the noise radar always has a much lower LPI than the conventional LFM radar. The noise radar's exceptional performance in the above evaluations indicates that it a suitable radar system for a variety of applications.

References

[1] Xu, X. and Narayanan, R. M.(2003). Impact of Different Correlation Receiving Techniques on the Imaging Performance of UWB Random Noise, *Geoscience & Remote Sensing Symposium,*

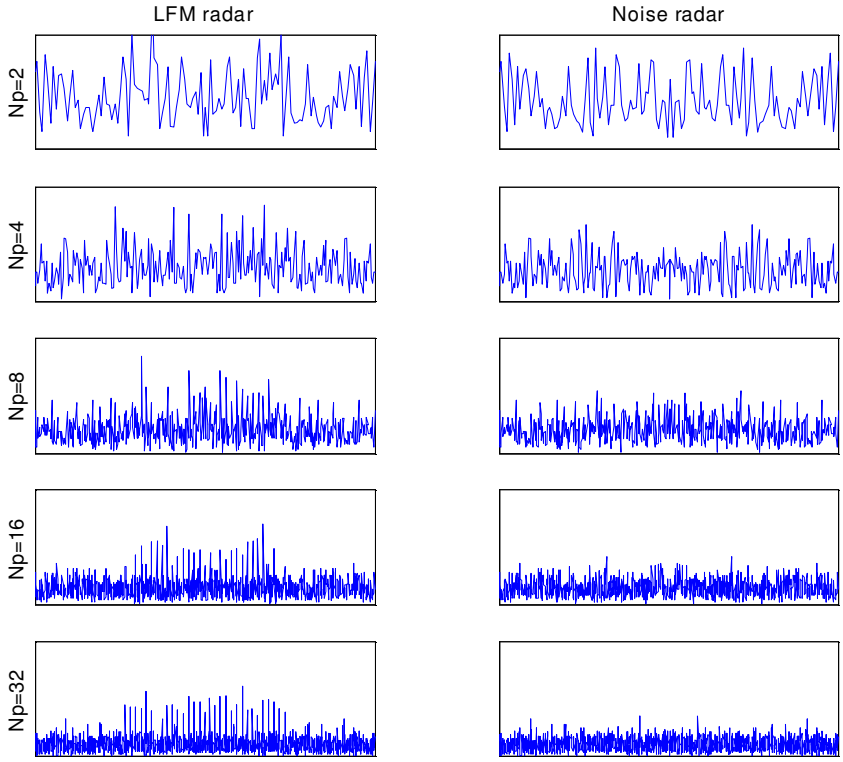

Fig. 9. Fourier spectrum of the observed signal in the case of a conventional LFM radar (left) and a NR (right) for various observation times. N_p is the number of radar pulses within the observation time. The signal to noise ratio is -6 dB.

IGARSS'03, Toulouse, France, Vol. 7, pp. 4,525-4,527.

[2] Lukin, K. A. (2002). Developments of Noise Radar Technology in LNDES IRE NASU, First International Workshop on the Noise Radar Technology, *NTRW 2002 Proceedings,* pp. 90-96, Yalta, Ukraine.

[3] Axelsson, S. R. J. (2000). On the Theory of Noise Doppler Radar, Geoscience and Remote Sensing *Symposium Proceedings 2000,* pp. 856-860, Honolulu, USA.

[4] Axelsson, S. R. J. (2003). Noise Radar For Range/Doppler Processing and Digital Beamforming Using Low-Bit ADC, *IEEE Trans. on Geoscience and Remote Sensing,* Vol. 41, No. 12, pp. 2,703-2,720.

[5] Horton, B. M. (1959). Noise-Modulated Distance Measuring Systems, *Proceedings of the IRE,* Vol. 47, pp. 821-828.

[6] Lukin, K. A. (2002). The Principles of Noise Radar Technology, First International Workshop on the Noise Radar Technology, *NTRW'2002 Proceedings,* pp. 13-22, Yalta, Ukraine.

[7] Bell, D. C. and Naryanan, R. M. (2001). Theoretical Aspects of Radar Imaging Using Stohastic Waveforms, *IEEE Trans. on Signal Processing,* Vol. 49, No. 2, pp. 394-400.

[8] Stephan, R. and Loele, H. (2000). Theoretical and Practical Characterization of a Broadband Random Noise Radar, *Dig. 2000 IEEE MTT-S International Microwave Symp.,* pp. 1,555-1,558, Boston, MA.

[9] Guosui, L., Hong, G., and Weimin, S. (1999). Development of Random Signal Radars", *IEEE Trans. on Aerospace and Electronic Systems,* Vol. 35, No. 3, pp. 770-777.

[10] Kalinin, V. I., Lyubchenko, V. E., and Panas, A. I. (2005). Wideband wireless communication with spectral processing of noise continuous waveform, *Proceedings XXVIIIth General Assembly of International Radio Science Union URSI-GA,* CD-ROM, New Delhi, India.

[11] Liu, G. and Gu, H. (1997). The present and the future of random signal radars, *IEEE Aerospace and Electronics Systems Magazine,* Vol. 12, No. 10, pp. 35-40.

[12] Liu, G., Gu, H., and Su, W. (1999). The development of random signal radar. *IEEE Transaction on Aerospace and Electronic Systems,* Vol. 35, No. 3, pp. 770-777.

[13] Cooper G. R. and McGillem, C. D. (1967). Random signal radar, Purdue Univ., West Lafayette, IN, Final Report.

[14] Guosui, L., Xiangquan, S., Jinhui, L., Guoyu, Y., and Yaoliang, S. (1991). Design of noise FW-CW radar and its implementation, *Proc. Inst. Elect.*

Eng. Radar Signal Process., Vol. 138, No. 5, pp. 420-426.

[15] Narayanan, R. M., Xu, Y., Hoffmeyer, P. D., and Curtis, J. O. (1998). Design, performance, and implementation of a coherent ultrawideband random noise radar, *Opt. Eng.,* Vol. 37, No. 6, pp. 1,855-1,869.

[16] Lukin, K. A. (1998). Millimeter wave noise radar technology, *Proc. 3rd Int. Kharkov Symp.,* Physics Engineering illimeter and Submillimeter-Waves, Kharkov, Ukraine, pp. 94-97.

[17] Theron, I. P., Walton, E. K., Gunawan, S., and Cai, L. (1999). Ultrawide-band noise radar in the VHF/UHF band, *IEEE Trans. Antennas Propagat.,* Vol. 47, No. 6, pp. 1,080-1,084.

[18] Theron, I. P., Walton, E. K., and Gunawan, S. (1998). Compact range radar cross-section measurements using a noise radar, *IEEE Trans. Antennas Propagat.,* Vol. 46, No. 9, pp. 1,285-1,288.

[19] Garmatyuk, D. S. and Narayanan, R. M. (2002). Ultra-wideband continuouswave random noise arc-SAR, *IEEE Trans. Geosci. Remote Sensing,* Vol. 40, No. 12, pp. 2,543-2,552.

[20] Narayanan, R. M. and Dawood, M. (2000). Doppler estimation using a coherent ultra wideband random noise radar, *IEEE Trans. Antennas Propagat.,* Vol. 48, No. 6, pp. 868-878.

[21] Xu, X. and Narayanan, R. M. (2001). FOPEN SAR imaging UWB step-frequency and random noise waveforms, *IEEE Trans. Aerosp. Electron. Syst.,* Vol. 37, No. 4, pp. 1,287-1,300.

[22] Xu, X. and Narayanan, R. M. (2001). Three-dimensional interferometric ISAR imaging for target scattering diagnosis and modeling, *IEEE Trans. Image Processing,* Vol. 10, No. 7, pp. 1,094-1,102.

[23] Xu, Y., Narayanan, R. M., Xu, X., and Curtis, J. O. (2001). Polarimetric processing of coherent random noise radar data for buried object detection, *IEEE Trans. Geosci. Remote Sensing,* Vol. 39, No. 3, pp. 467-478.

[24] Xu, X. and Narayanan, R. M. (2001). Range sidelobe suppression technique for coherent ultra-wideband random noise radar imaging, *IEEE Trans. Antennas Propagat.,* Vol. 49, No. 12, pp. 1,836-1,842.

[25] Lai, C. P., Narayanan, R. M. Culkowski, G. (2006). Through wall surveillance usig ultrawide-band random noise radar, *25 th Army Science Conference,* Florida, November 27-30, Orlando, Florida, pp. 1-4.